HEAVY-ION RADIOGRAPHY AND HEAVY-ION COMPUTED TOMOGRAPHY[1,2]

Jacob I. Fabrikant, M.D., Ph.D.[3,4]
Donner Laboratory
University of California, Berkeley
Lawrence Berkeley Laboratory
Berkeley, California

and

William R. Holley, Ph.D, Eric W. McFarland,
and Cornelius A. Tobias, Ph.D.
Division of Biology and Medicine
Lawrence Berkeley Laboratory
Berkeley, California

LBL--14001

DE82 012537

[1]Presented at Scientific Session, Third International Symposium of Radiation Protection-Advances in Theory and Practice, Inverness, Scotland, June 6-11, 1982

[2]This work was supported by the Office of Health and Environmental Research of the U.S. Department of Energy under Contract Number DE-AC03-76SF00098.

[3]Professor of Radiology, University of California School of Medicine, San Francisco, California

[4]Mailing address: Donner Laboratory, University of California, Berkeley, California 94720.

HEAVY-ION RADIOGRAPHY AND HEAVY-ION COMPUTED TOMOGRAPHY

J I Fabrikant, W R Holley, E W McFarland, C A Tobias
Lawrence Berkeley Laboratory
Donner Laboratory, University of California, Berkeley, CA 94720
University of California School of Medicine, San Francisco, CA

INTRODUCTION

Heavy-ion projection radiography and computerized tomography (CT) are being developed at Lawrence Berkeley Laboratory into low-dose, safe, reliable, non-invasive radiological procedures that quantitate and image very small density differences in human tissues (1,2). It is this ability of heavy ions to achieve a more precise resolution of density and composition of normal and neoplastic tissues than do x-rays that provide the potential for improved clinical detection of small cancers in human tissues. Heavy-ion nuclear track detector systems provide the basis for improved quantitative densitometry in tissues and organs, for projection imaging, and for 2- and 3-dimensional CT reconstructions with precise stopping power values (3). This report provides an overview of heavy-ion imaging applied to medicine at Lawrence Berkeley Laboratory, and illustrates its potential in the investigation of problems in diagnostic roentgenology. These include advantage of higher sensitivity of particle imaging with lower patient dosage compared with x-rays (eg, heavy-ion mammography), measurement of residual range for determination of 2- and 3-dimensional electronic density distribution (eg, heavy-ion CT of brain).

PROCEDURE OF HEAVY-ION RADIOGRAPHY

The BEVALAC facility (4) at Lawrence Berkeley Laboratory can accelerate fully stripped atomic nuclei from carbon (Z=6) to krypton (Z=34); useful ranges in tissue of 40 cm or more are available. Heavy-ion radiography has been done with beams of helium-4, carbon-12, oxygen-16, and neon-20 at different energies. The method uses thin plastic nuclear track detectors (eg, Lexan or cellulose nitrate) originally developed for space research to study heavy primary cosmic rays and to record tracks due to nuclear fission fragments. Fig 1 illustrates the technique of heavy-ion (eg, carbon ions) radiography (5). A parallel monoenergetic beam of heavy ions passes through the object to be radiographed and stops in a stack of some 25 to 100 plastic detector sheets, thereby recording the exact position and depth of each

stopping heavy ion. The particles of sufficiently high LET produce a latent lesion in the plastic foil that is developed with concentrated NaOH to form a microscopic tapered hole. The stopping point distribution in the detector stack corresponds to the residual range distribution of the particles after crossing the object; therefore, the plastic stacks indirectly measure the stopping power distribution in the radiographed object. The information in the detector stack is then processed; the information on location and residual range is transferred by an optical scanning method to a computer for analysis and image display.

COMPUTER SYNTHESIS AND IMAGE DISPLAY

Individual nuclear track detector foils are dark field illuminated and scanned with a Vidicon (Hamamatsu) camera; the signal from the camera is then digitized by a high-speed analog-to-digital converter. The computer (VAX 11-780) is used to calculate the average distance particles penetrate into the stack; these values are used for further processing and image display. From the residual range in the stack the total range of the particles can be determined at each lateral point (pixel location). The ratio of the range of particles passing through water, Rw, is related to the stopping power values by the following $Rw/Rs = [\overline{\mu_S/\mu_W}]$ where μ_S and μ_W are the linear stopping power values in the tissue and water respectively, and the quantities are averaged along the particle path in the tissue. The heavy-ion number (τ) is defined similarly to the Hounsfield unit (H) for x-ray images: $\tau=1000\ (\overline{\mu_S/\mu_W} - 1)$, where μ_S and μ_W are average electronic stopping powers in the tissue and water respectively.

APPLICATIONS TO MEDICINE

Considerable work has been done in our laboratory on the physical and accelerator beam aspects of heavy-ion radiography, on detector characteristics and response, on image resolution and radiation dose, computer analysis and image display, and 2- and 3-dimensional reconstruction (1-10). The following is a brief overview of two heavy-ion imaging procedures on patients, illustrating the applications of heavy-ion mammography and heavy-ion computerized tomography of the brain.

HEAVY-ION MAMMOGRAHY

The improved density resolution of heavy-ion mammography over x-ray mammography and xeroradiography provides the potential for identifying small breast cancers of less than 1 cm in diameter at lower dose than do x-rays. The results of the initial clinical trial of heavy-ion mammography are promising, and warrant continued study for application to the early diagnosis of breast cancer in women (7-9). Patient studies are done at the Lawrence Berkeley Laboratory BEVALAC; the patient lies prone in the beamline on a specially designed mammography table. The breast to be examined is immersed in a rectangular lucite water bath, and is gently compressed (either in the lateral or in the cephalocaudad

direction, depending on the radiographic projection) between parallel plastic plates. The water-bath assembly is positioned perpendicular to the heavy-ion beam line. The patient is shielded by brass-blocks and beam collimation. The detector stack is mounted on the downstream side of the water-bath assembly perpendicular to the beam. A single beam pulse at 0.5 sec is used, eg, carbon-12 ions, 250 MeV/amu, fluence of 10^3 to $2x10^4$ particles/cm^2, radiation dose of less than 50 mrems, which is sufficient to expose a detector stack of about 25 detector sheets. Two heavy-ion mammograms (lateral and cephalocaudad) are taken of each breast. The procedure (patient positioning and radiographic exposures) requires 30 to 40 min.

Thus far, 39 clinical breast cancer patients have been examined; over 160 heavy-ion mammograms have been obtained and compared with the x-ray mammograms or xeroradiographs, and with pathological findings where available (8). Heavy-ions demonstrate almost all abnormal densities in the breasts of patients that could be detected by x-rays. Density resolution in heavy-ion mammograms exceeds that of the x-ray mammography. X-rays provide improved spatial resolution, and are relatively more sensitive to higher atomic number tissue structures. In all but two of the 39 patients examined, heavy-ion mammography confirmed the x-ray studies, eg, either positive or negative for breast cancer. Biopsy studies verified these findings in 12 patients (7 benign and 4 malignant tumors); 25 patients did not have biopsies done. In one patient with a <1 cm nonpalpable breast mass demonstrated on carbon-ion and not on x-ray mammograms, the breast biopsy proved to be carcinoma. In the other patient with a <1 cm nonpalpable mass demonstrated only on the carbon-ion mammogram, the breast biopsy proved to be a benign tumor.

Analysis of heavy-ion mammographic data is accomplished on a VAX 11-780 computer system. Algorithms have been developed to process the density information and present it in useful imaging formats. In addition to a gray scale mammogram (Fig 2) produced for each patient exposure, the analysis generates isodensity contour plots (Fig 3) and heavy-ion number (τ) frequency histograms (Fig 4) for correlation with radiological images and pathological specimens. The isodensity contour plot is a quantitative representation connecting regions of constant integrated electronic stopping power. The composite contour plot outlines the size and structure of the breast lesion and gives information on the parenchymal patterns of the breast tissues. We plan to use this for assessing the potential for developing cancer in a procedure analogous to that used in the analysis of x-ray mammograms for classifying the potential risk of developing cancer of the breast.

The stopping power frequency distribution (Fig 4) provides important quantitative information; tissue studies (10) show

that the stopping power values and heavy-ion numbers (τ) for normal, neoplastic and dysplastic breast tissues are different. The heavy-ion mammogram frequency distribution histo gram of τ provides a measure of the relative quantities of the different types of tissues present in the breast. Fig 4 demonstrates a large peak of normal breast tissue at τ=-43, and a smaller peak at τ=0, indicating pathological dense breast tissue, possibly cancer. Methods are now being developed to interpret these heavy-ion (τ) number frequency distribution histograms for each individual breast cancer patient. The method will be of value in test-retest clinical studieswhere measurable changes in the stopping value distribution may be quantified and correlated with pathological changes.

HEAVY-ION COMPUTERIZED TOMOGRAPHY

Heavy-ion radiography has proved to be very suitable for 2-dimensional CT image reconstruction (2,3). The passing or stopping of all individual heavy particles are recorded, and the sensitivity for stopping power measurements is high. Heavy-ion CT reconstructions of high quality are obtained at relatively low radiation dose. Successful CT reconstructions of various imaging phantoms, of a rat's head, a human spine, and of the human brain in specimens and patients have been achieved (5).

For 2-dimensional heavy-particle CT reconstruction, the heavy-ion beam is passed through a horizontal slit. Between each successive beam pulse the patient or specimen is rotated to different angles of incidence while the nuclear plastic detector stack is indexed vertically. The images formed in the stack by a sequence of beam pulses appear as narrow bands at specified angles of incidence and do not overlap. (5,6).

A heavy-ion CT scanning system suitable for patients or human organ specimens has been constructed. With this device we have obtained the coronal heavy-ion CT images of a human brain specimen shcwn in Fig 5. Ninety projections (2^{o} intervals through a total rotation of 180^{o}) were obtained using neon-ion beam (557 MeV/amu) with a slit width of 1.5 mm. This neon-ion CT reconstruction demonstrates high resolution of the soft tissue structures of the brain. Spatial resolution does not limit the precise delineation of internal structures of the brain. Density resolution appears better than in the comparison x-ray CT image. In the neon-ion CT, differences in density can be determined between the regions of the white and gray matter, of the cerebral cortex, and the structures of the mid-brain, the corpus collosum, the anterior commissure, the lateral ventricles and the third ventricle, the fornix, and the region of the optic chiasm.

Fig 6 illustrates the first neon-ion (670 MeV/amu) CT reconstruction of the brain in a patient with metastatic melanoma to the cerebral cortex. The heavy-ion CT is a 2-dimensional 1.5 mm-

thick section through a 3-dimensional 7.5 cm thick solid cylinder cut through the center of the brain. While this initial study lacks the high resolution of tissue structure of the brain compared with x-ray CT, no corrections have been made of this image for tissue or computational artifacts, and only 30 projection angles have been used. Nevertheless, delineation of the internal structures of the brain and density resolution appears at least similar to the early NMR and x-ray CT brain scans. Differences in density can be determined between various regions of skull and in brain structures.

SUMMARY

Heavy-ion projection and CT radiography is being developed into a safe, low-dose, noninvasive radiological procedure that can quantitate and image small density differences in human tissues. The applications to heavy-ion mammography and heavy-ion CT imaging of the brain in clinical patients suggest their potential value in cancer diagnosis.

ACKNOWLEDGEMENTS

The authors thank Mrs. Kathleen Becky and Mr. Robert Stevens for help with preparation of the manuscript and illustrations. Research supported by US NIH/NCI CA YO1-CB-40302 and U.S. Department of Energy under contract No. DE-AC03-76SF00098.

REFERENCES

(1) Benton EV, Henke RP, Tobias CA. Science 182:474-476, 1973. (2) Tobias, CA, Benton EV, Capp MP. In: Recent Advances in Nuclear Medicine 5:71-102, 1978. (3) Tobias CA, Fabrikant JI, Benton EV, Holley WR. In: Biological and Medical Research with Accelerated Heavy Ions at the BEVALAC 1977-1980 (Pirruccello MC and Tobias CA, eds), pp 335-346. Lawrence Berkeley Laboratory Report LBL-11220, 1980. (4) Pirruccello MC, Tobias CA, eds. Biological and Medical Research with Accelerated Heavy Ions at the BEVALAC, 1977-1980. Lawrence Berkeley Laboratory Report LBL-11220, 1980. (5) Holley WR, Henke RP, Gauger GE, Jones B, Benton EV, Fabrikant JI, Tobias CA. In: Sixth Computer Radiology IEEE Trans. 64-70, 1979. (6) Holley WR, Tobias CA, Fabrikant JI, Llacer J, Chu WT, Benton EV, Soc Photo-Opt Instrum Eng 273:280-393, 1981. (7) Fabrikant JI, Tobias CA, Capp MP, Benton EV, Holley WR. Soc Photo-Opt Instrum Eng 233: 255-263, 1980. (8) Fabrikant JI, Tobias CA, Capp MP, Holley WR, Woodruff KH, Sickles, EA. In: Biological and Medical Research with Accelerated Heavy Ions at the BEVALAC 1977-1980 (Pirruccello MC, Tobias CA, eds), pp. 347-358. Lawrence Berkeley Laboratory Report LBL-11220, 1980. (9) Sickles EA, Benton, EV, Tobias CA, Woodruff KH. In: Reduced Dose Mammography, pp. 501-505, Masson, 1979. (10) Sommer FG, Capp MP, Tobias CA, Benton EV, Woodruff KH, Henke RP, Holley WR, Genant HK. Invest Radiol 13:163-170, 1978.

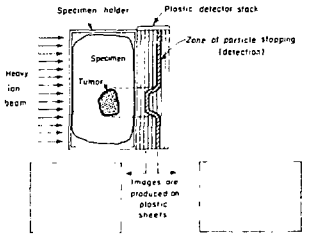

Figure 1

Figure 2

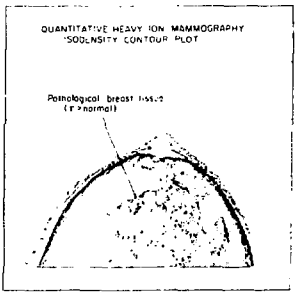

Figure 3

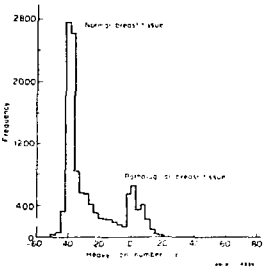

Figure 4

Figure 5

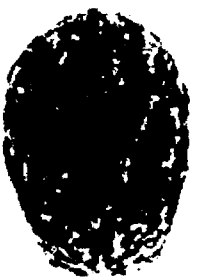

Figure 6

XBB 822-1651